

Nuclear Spin Absorption Spectra in Solids

A. G. ANDERSON

International Business Machines Research Laboratory, San Jose, California

(Received October 5, 1961)

Nuclear magnetic spin absorption spectra in both parallel and perpendicular ac and dc magnetic fields are reported for lithium nuclei in lithium metal. This is a case where the predominant interactions are the Zeeman interaction of the nuclear magnetic moment with the dc field and the magnetic dipole-dipole interaction between nuclei in fixed lattice positions. For an applied dc field, H_0 , the spectrum consists of absorption around zero frequency, around $\omega = \gamma H_0$, and around $\omega = 2\gamma H_0$. Linewidths and relative amplitudes observed experimentally are in good agreement with the theory, which predicts linewidths of approximately

the same magnitude for all lines and line amplitudes which vary as H_0^{-4} , H_0^0 , or H_0^{-2} . At applied dc fields which are large compared with the internal magnetic dipole-dipole fields an additional absorption is observed for the parallel-field case at very low frequencies; this is attributed to the relatively long time required for establishment of internal equilibrium at these fields.

Absorption spectra are reported for lithium-magnesium alloys. In these alloys addition of magnesium produces electric quadrupole broadening of the lithium absorption spectra. The zero-field absorption spectrum of copper is also reported.

I. INTRODUCTION

IN a paramagnetic material, in small dc magnetic fields, energy can be absorbed from an ac magnetic field at a frequency of the order of T_1^{-1} , which characterizes the spin-lattice relaxation phenomena with time constant T_1 , or at a frequency of the order of T_2^{-1} , which characterizes the internal relaxation phenomena. We will be concerned here with a situation where T_1 is long and consider only absorption around T_2^{-1} , which, in agreement with past practice, we call "spin absorption." The experimental systems investigated were those of nuclear magnetic moments in the metals lithium, lithium-magnesium, and copper.

The history of spin absorption spectra in magnetic dipole systems having magnetic dipole-dipole interactions between neighbors dates back to early work of Waller,¹ who treated the problem for zero external magnetic field. Here absorption occurs over a range of frequencies determined by the distribution of internal local fields at the magnetic sites. Waller found that the ac susceptibility was equal to the low-frequency susceptibility as long as the applied frequency was small compared with that determined by the rms interaction energy between spins. In a concentrated paramagnetic salt the latter frequency is of the order of 10^9 cps, while in the nuclear magnetic case it is of the order of 10^4 cps. It is important to emphasize that these frequencies characterize absorption of energy in the dipole-dipole coupled system without reference to the lattice, except for the weak coupling which produces spin-lattice relaxation and which can ordinarily be accounted for separately or completely neglected; the spin system is regarded here as an isolated system, having interactions with an ac magnetic field and having a distribution of populations established by interactions between neighbors and characterized by a single spin temperature.

Early work by Gorter² and others on paramagnetic

salts showed that such zero-field absorption in the spin system did occur. This work was in the low-frequency end of the absorption spectrum and characterized the rms interaction between the spins only by the magnitude and field dependence of the absorption, under the assumption of a particular zero-field distribution function. The results, however, were sufficient to indicate zero-field line narrowing due to exchange interaction³ in some of the copper salts.

Broer⁴ considered the theoretical problem for the cases of nonzero dc field. He found that absorption occurs with either parallel (\parallel) orientation of the oscillating ac field and the static dc field or with perpendicular (\perp) orientation of these fields. In each case he showed that absorption occurs around zero frequency, around the Larmor frequency, and around double the Larmor frequency. The absorptions at other than the Larmor line, $\gamma H_0(\perp)$, arise from matrix elements of the dipole-dipole Hamiltonian and consist of spectra which decrease in intensity, relative to $\gamma H_0(\perp)$, as some inverse-squared power of the applied dc field. The lines other than $\gamma H_0(\perp)$ or $\gamma H_0(\parallel)$ arise from double spin-flip processes where two neighboring spins flip, with respect to quantization of angular momentum along the applied dc field direction, in either the same or opposite directions. The case of opposite spin flips gives the zero frequency, $0\gamma H_0(\perp)$ or $0\gamma H_0(\parallel)$, line, which has been a subject of considerable experimental interest in the past.^{2,5} In the limit of high field, only the Larmor line should be observed, the other lines being generally of insufficient intensity. There have been indications that the $2\gamma H_0(\parallel)$, $\gamma H_0(\parallel)$, and $2\gamma H_0(\perp)$ lines have been seen in some of the electron paramagnetic systems.^{6,7} These data are,

³ C. J. Gorter and J. H. Van Vleck, *Phys. Rev.* **72**, 1128 (1947).

⁴ L. J. F. Broer, *Physica* **10**, 801 (1943).

⁵ A. Wright, *Phys. Rev.* **76**, 1826 (1949).

⁶ V. A. Kutuzov, *J. Exptl. Theoret. Phys.* **35**, 910 (1959); A. I. Kurushin, *ibid.* **32**, 766 (1957).

⁷ For example, the relative amplitude of the $2\gamma H_0(\perp)$ line at 9 kMc/sec as compared with the $\gamma H_0(\perp)$ line at 9 kMc/sec in ferric ammonium alum powder, kindly taken for the author by A. W. Hornig, agrees well with an internal field, $(10/3)(\Delta H)^2 = 450$ gauss². This, of course, neglects crystalline interactions and

¹ I. Waller, *Z. Physik* **79**, 370 (1932).

² See, for example, C. J. Gorter, *Paramagnetic Relaxation* (Elsevier Publishing Company, New York, 1947); C. J. Gorter, *Progress in Low Temperature Physics* (Interscience Publishers, Inc., New York, 1957), Vol. II, p. 267.

however, not very detailed, while previous work in nuclear systems has clearly shown the existence of these lines.⁸

Wright⁵ later considered in some detail the theory of the zero-frequency lines. These lines consist of the absorption spectra in which there is no change in Zeeman energy (two opposite spin flips) but where there is a change in the spin-spin energy of the system. Wright calculated the field dependence, amplitudes, and widths of both of these lines, although the calculations were of somewhat limited quantitative applicability for the parallel field case. In the perpendicular case, where the absorption decreases as H_0^{-2} , the available experimental data for the paramagnetic salts were in reasonable agreement with these calculations, particularly with respect to the field dependence and amplitude of the absorption. In the parallel field case, where absorption is expected to decrease as H_0^{-4} , little agreement between experiment and theory was found; the experimental work in the paramagnetic salts showed a complete lack of agreement with the expected field dependence of absorption. The nuclear systems reported here offer an exceptionally simple case for experimental study and comparison with this theory, and the data indicate the correctness of Wright's theory in both parallel and perpendicular field cases, except for very low frequency (~ 200 cps) in parallel field. Wright also obtained theoretical second and fourth moments for the zero-field line, for which experimental results have since been reported.⁸

More recently, Cheng⁹ has extended the theory to a calculation of the rms widths of the $\gamma H_0(\parallel)$, $2\gamma H_0(\parallel)$, and $2\gamma H_0(\perp)$ lines and has found that these lines are of approximately the same width as the Larmor line itself, as long as only Zeeman and dipole-dipole interactions are important. In the experimental data reported here, this is the case; the data appear to be in good agreement with theory.

When the possibility of an isotropic exchange interaction is included in the theory, the available calculations show^{5,9,10} that the $\gamma H_0(\perp)$ line is exchange narrowed, while the $0\gamma H_0(\perp)$, $\gamma H_0(\parallel)$, $2\gamma H_0(\perp)$, and $2\gamma H_0(\parallel)$ lines are broadened. Unfortunately, no check of this was possible with the systems reported here; experimental work on the paramagnetic salts¹¹ may yield interesting comparisons in the near future.

All of the theory mentioned has required, as a starting assumption, the description of the spin system by a spin temperature with an equilibrium ratio between Zeeman and dipole-dipole energy which is determined

is an oversimplification of the actual case. See, for more detailed analysis, J. Ubbink, J. A. Poulis, and C. J. Gorter, *Physica* **17**, 213 (1951), and P. H. E. Meyer, *ibid.* **17**, 899 (1951). The $2\gamma H_0(\perp)$ line has been seen in a number of cases in other materials, usually with complicating factors of exchange and crystal field interactions.

⁸ A. G. Anderson, *Phys. Rev.* **115**, 863 (1959).

⁹ H. Cheng, *Phys. Rev.* **123**, 1359 (1961).

¹⁰ J. H. Van Vleck, *Phys. Rev.* **74**, 1168 (1948).

¹¹ J. C. Verstelle (private communication).

by the external field H_0 and the internal dipole-dipole fields. On the other hand, arguments for and against the concept of a single spin temperature have had a long history: Kronig and Bouwkamp¹² gave a cogent argument against spin temperature equilibrium at high field, arguing that ready interchange of energy between dipole-dipole energy and Zeeman energy must be an extremely slow process at high field because of energy conservation requirements; a single Zeeman flip takes place in external field H_0 , while internal fields at the same spin have an exceedingly small probability of being of comparable magnitude for energy conservation if H_0 is large compared with the rms dipole-dipole fields. Broer⁴ took an opposite view, arguing partly on the basis of experimental evidence then available to him. This subject has been reopened recently¹³ and experimental demonstration of the increased absorption in parallel field at frequencies comparable with the inverse time for equilibrium between dipole-dipole and Zeeman systems has been reported for the electron paramagnetic case.¹⁴ Similar results for the nuclear case are reported here.

Finally, broadening of lines^{15,16} occurs in dilute alloys of cubic metals, such as lithium, because the local environment of the lithium nuclei around the impurity nuclei is noncubic; this noncubic environment, which arises from both charge and strain effects, produces a nonspherically symmetrical electric field at the lithium site and thus an interaction¹⁵ with the electric quadrupole moment of the lithium nucleus. In lithium-magnesium alloys the electric quadrupole contributions to the spectra are of the same order of magnitude as the dipole-dipole contributions, resulting in lines which change in shape and width with increasing Mg concentration. The low-field data reported here are in agreement with the data of Sukenik¹⁶ at high field.

The experimental method used here relies on the long relaxation times which can be obtained at low temperatures in nuclear magnetic systems; the temperature is chosen to provide a T_1 of several seconds. A large dc field is applied for a period long enough to establish an equilibrium polarization, followed by adiabatic demagnetization to low field where the nuclear system is heated by absorption of energy from an ac field, and finally, return of the dc field to its high-field value and measurement of the magnetization, which is equivalent to measurement of spin energy or

¹² R. Kronig and C. J. Bouwkamp, *Physica* **5**, 521 (1938).

¹³ N. Bloembergen *et al.*, *Phys. Rev.* **114**, 445 (1959); J. C. Verstelle, G. W. J. Drewes, and C. J. Gorter, *Physica* **24**, 632 (1958); W. J. Caspers, *ibid.* **24**, 778 (1960).

¹⁴ P. R. Locher and J. C. Verstelle, *Proceedings of the Seventh International Conference on Low-Temperature Physics* (University of Toronto Press, Toronto, 1961), p. 56.

¹⁵ M. H. Cohen and F. Rief, in *Solid-State Physics*, edited by F. Seitz and D. Turnbull (Academic Press, Inc., New York, 1957), Vol. 5, p. 331.

¹⁶ N. Bloembergen and T. J. Rowland, *Acta Met.* **1**, 731 (1953); H. J. Sukenik, thesis, University of California, Berkeley, 1958 (unpublished).

spin temperature. If the adiabatic demagnetization-absorption-remagnetization-measurement cycle is completed in a time short compared with T_1 , then the high-field measurement provides a measure of the low-field absorption.^{8,17} The total range of frequencies required to investigate the multiple line structure of the low-field absorption extends from zero to about 100 kc/sec for the nuclear systems; this allows detailed investigation of the absorption structure with simpler experimental apparatus than that necessary in the equivalent electron paramagnetic case.

Preliminary reports of some parts of this work have appeared elsewhere.¹⁸

II. THEORY

The Hamiltonian⁵ for a spin system with magnetic dipole-dipole interactions between neighbors and with Zeeman interactions with an external field H_0 is given by

$$\begin{aligned}
 H &= -g\beta H_0 \sum_i I_{zi} \\
 &\quad + \sum_{i>j} g^2 \beta^2 r_{ij}^{-3} \left[\mathbf{I}_i \cdot \mathbf{I}_j - \frac{3(\mathbf{r}_{ij} \cdot \mathbf{I}_i)(\mathbf{r}_{ij} \cdot \mathbf{I}_j)}{r_{ij}^2} \right] \\
 &= H_0 + H_3 + H_4 + H_5 + H_6, \\
 H_0 &= -g\beta H_0 \sum_i I_{zi} + \sum_{i \neq j} A_{ij} \mathbf{I}_i \cdot \mathbf{I}_j + \sum_{i \neq j} C_{ij} I_{zi} I_{zj}, \\
 H_3 &= \sum_{i \neq j} D_{ij} I_{+i} I_{+j}, \quad H_4 = H_3^*, \\
 H_5 &= \sum_{i \neq j} E_{ij} I_{+i} I_{zj}, \quad H_6 = H_5^*; \\
 A_{ij} &= \frac{1}{2} [g^2 \beta^2 r_{ij}^{-3} (3\gamma_{ij}^2 - 1)], \\
 C_{ij} &= -\frac{1}{2} [g^2 \beta^2 r_{ij}^{-3} (3\gamma_{ij}^2 - 1)] = -A_{ij}, \\
 D_{ij} &= -\frac{3}{8} [g^2 \beta^2 r_{ij}^{-3} (\alpha_{ij}^2 - \beta_{ij}^2 - 2i\alpha_{ij}\beta_{ij})], \\
 E_{ij} &= -\frac{3}{2} [g^2 \beta^2 r_{ij}^{-3} \gamma_{ij} (\alpha_{ij} - i\beta_{ij})].
 \end{aligned}
 \tag{1}$$

The radius vector between spins is r_{ij} ; α_{ij} , β_{ij} , and γ_{ij} are direction cosines of r_{ij} with respect to axes x , y , z ; g is the nuclear g factor; β is the nuclear magneton; and the asterisk denotes the Hermitian conjugate. The H_0 Hamiltonian is the usual high-field truncated Hamiltonian,¹⁰ while H_3 , H_4 , H_5 , and H_6 are terms usually neglected at high field.

When this system is in equilibrium with the lattice, the energy is given by

$$\begin{aligned}
 E = \langle H \rangle &= \chi_0 [H_0^2 + (5/3) \langle (\Delta H)^2 \rangle] \\
 &= \chi_0 T_s^{-1} [H_0^2 + (5/3) \langle (\Delta H)^2 \rangle], \tag{2}
 \end{aligned}$$

¹⁷ N. F. Ramsey and R. V. Pound, Phys. Rev. **81**, 278 (1951).

¹⁸ A. G. Anderson, *Proceedings of the Seventh International Conference on Low-Temperature Physics* (University of Toronto Press, Toronto, 1961), p. 59.

where χ_0 is the susceptibility at 1°K, given by

$$\chi_0 = N g^2 \beta^2 I(I+1) / (3k); \quad \langle (\Delta H)^2 \rangle = \frac{2}{3} g^2 \beta^2 I(I+1) \sum_i r_{ij}^{-6}$$

is the Van Vleck second moment of the Larmor line; and T_L is the lattice temperature in degrees Kelvin. (The high-temperature approximation, where $g\beta H_0 \ll kT_L$, is valid in the range of experiments reported here.) When the system is in internal equilibrium, but not necessarily in equilibrium with the lattice, we make the assumption of an internal spin temperature and characterize the system by

$$E_s = \langle H \rangle = \chi_0 T_s^{-1} [H_0^2 + (5/3) \langle (\Delta H)^2 \rangle],$$

where now T_s^{-1} is the spin temperature. The use of T_s is generally a good approximation, except for cases to be discussed where the rate of approach to internal equilibrium is slow.

In order to obtain either parallel or perpendicular absorption spectra at frequency ν , it is necessary to calculate, from this Hamiltonian, the magnetic moment matrix element, $M(\nu)_{kl}$, for the transitions linking states k and l , differing in energy by $h\nu$. As discussed by Broer,⁴ the distribution function $f(\nu)$ is obtained from

$$f(\nu) \Delta\nu = \sum_{\nu-\Delta\nu/2}^{\nu+\Delta\nu/2} |M_{kl}|^2.$$

Details of the absorption spectrum are then obtained by calculating various moments of $f(\nu)$; for example, the zeroth moment is given by

$$\int_0^\infty f(\nu) d\nu = \text{Tr}(M^2).$$

Broer and Wright calculated the zeroth, second, and fourth moments of the zero-field line.

At nonzero dc field, the ac field contributes either a term $2g\beta \sum I_x H_1 \cos\omega t$ or a term $2g\beta \sum I_z H_1 \cos\omega t$ to the Hamiltonian (1). In first-order time-dependent perturbation theory, using only the H_0 and the ac contributions to the Hamiltonian, $M = g\beta \sum I_x$ and $f(\nu)$ consists of only one line centered at the Larmor frequency. When the contributions of the other parts of (1) are considered by perturbation theory, with H_0 as the starting Hamiltonian, then lines are also found at $0\gamma H_0(\perp)$, $0\gamma H_0(\parallel)$, $2\gamma H_0(\perp)$, and $2\gamma H_0(\parallel)$. Higher-order perturbation calculations determine widths of these lines and indicate the presence of the line $0\gamma H_0(\parallel)$ and higher frequency lines at $3\gamma H_0$. A number of these calculations have been made. Most recently, Cheng⁹ has calculated the second moments of the $\gamma H_0(\parallel)$, $2\gamma H_0(\perp)$, and $2\gamma H_0(\parallel)$ lines. He has also obtained general formulas for calculating other line amplitudes and moments.

We may write⁹ the magnetic moment for a particular

transition by considering the general formula,

$$M_i = \sum_{i_1, i_2, \dots, i_n} \frac{(H_{i_1}, (H_{i_2}, (\dots (H_{i_n} M_{0s}))))}{(\Delta E_{i_1})(\Delta E_{i_1} + \Delta E_{i_2}) \dots (\Delta E_{i_1} + \Delta E_{i_2} + \dots + \Delta E_{i_n})}, \quad (3)$$

where

$$\sum_{j=1}^n (\Delta I_z)_{ij} = \Delta I_{zi}$$

is required. In this formula M_{0s} is the rf perturbation magnetic moment (e.g., $g\beta \sum I_{zi}$) either perpendicular or parallel to the dc magnetic field and H_{i_n} are the various partial Hamiltonians from (1). The high field approximation is assumed, where H_0 is the starting Hamiltonian with energy levels E_i ; n the order of perturbation involved, and ΔI_{zi} gives the required change in spin orientation (single flip, double flip, etc.) to account for the line involved. For example, the second Larmor line in perpendicular field requires $\Delta I_z = 2$ and $n = 1$, which gives

$$M_{2(\perp)} = (H_0, \frac{1}{2} g\beta I_-) / g\beta H_0.$$

Once one has M_i , then $\int f_i(\nu) d\nu = \text{Tr} M_i^2$; this is now the zeroth moment of the i th line separated from other lines and demonstrates the simplicity of (2) as compared with other developments. Higher moments also follow readily, as discussed by Cheng.

A summary of the theoretical results may be found in Table I, where present experimental results are also listed. A discussion of the experimental work will be found in later sections.

When quadrupole interactions are included¹⁹ in (1), a term, H_Q , must be added:

$$H_Q = \sum_{i=1}^N \left[\frac{3}{2} (I_{ij} I_{ik} + I_{ik} I_{ij}) - \delta_{ij} I_i^2 \right] (V_i)_{jk} \left(\frac{eQ}{6I(2I-1)} \right), \quad (4)$$

where j, k signify x, y, z components of I_i ; V_i is the electrostatic potential at i ; and $(V_i)_{xy} = \partial^2 V_i / \partial x \partial y$ is the xy component of the field gradient. The zero-field absorption spectrum is broadened by this interaction to give a total zero-field second moment¹⁹ of

$$\begin{aligned} \langle (\Delta\nu)^2 \rangle &= \langle (\Delta\nu)^2 \rangle_{ad} + \langle (\Delta\nu)^2 \rangle_Q \\ &= (10/3) \langle (\Delta H)^2 \rangle (\gamma/2\pi)^2 + (10/3) (3/200) \\ &\quad \times \left(\frac{e^2 Q^2}{h^2} \frac{4I(I+1) - 3}{I^2(2I-1)^2} \frac{1}{N} \sum_i \sum_{jk} (V_i)_{jk}^2 \right) \\ &= (\gamma/2\pi)^2 (10/3) \langle (\Delta H)^2 \rangle_{\text{eff}}. \end{aligned} \quad (5)$$

This result is valid for a powder, which was used here. A similar result holds for the $\gamma H_0(\perp)$ line, with $\langle (\Delta\nu)^2 \rangle$ reduced by the usual three-tenths. The field depend-

ences of other lines are also affected; these are given¹⁹ by replacing $\langle (\Delta H)^2 \rangle$ in Table I by $\langle (\Delta H)^2 \rangle_{\text{eff}}$.

The assumptions made by Brown in this calculation are that the Zeeman energy is large in comparison with both dipole-dipole and quadrupole energies and that the quadrupole interaction energy is not large in comparison with the dipole-dipole energy. The first assumption is the usual "high-field" approximation. The second assumption assures that it will be possible to maintain a uniform spin temperature throughout the spin system. When dipole-dipole and quadrupole energies are comparable, then spin diffusion is not inhibited, and one expects rapid internal equilibrium.¹³ The argument is similar to arguments used in considering questions of equilibrium in an applied dc magnetic field, without quadrupole interactions. In any event, the Li-Mg alloys reported here have quadrupole interactions which are small and the spin temperature approximation is expected to be valid; the experimental evidence verifies this assumption.

III. EXPERIMENTAL METHOD

Since many of the details of the experimental method have been discussed previously,^{8,17,20} only a brief discussion, including details not previously reported, will be given here.

The experimental method is shown in Fig. 1. The spin system is brought into equilibrium with the lattice during a time long compared with T_1 . The system is then adiabatically demagnetized to a field, H_0 , where

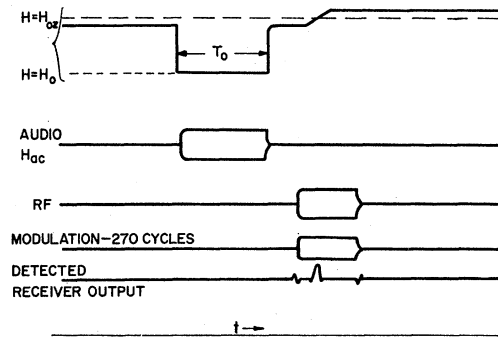


FIG. 1. Experimental method. During the initial high-field period, the spin system comes into equilibrium with the lattice at spin temperature $T_s = T_L$. At the start of the T_0 period the dc field H is adiabatically lowered to H_0 ; the low-field spin absorption occurs during the time interval T_0 . At the conclusion of T_0 , H is adiabatically raised to H_{0z} and the spin system energy is measured. The absorption of energy at dc field H_0 during interval T_0 is determined by the amplitude of the observed signal at field H_{0z} .

¹⁹ L. Brown, IBM Research Laboratory, San Jose, California, memorandum RJM-001, 1959 (unpublished).

²⁰ A. G. Anderson and A. G. Redfield, Phys. Rev. **116**, 583 (1959).

TABLE I. Spin absorption spectra.

Line of interest	Theory	$\int f(\nu)d\nu$	$\langle(\Delta\nu)^2\rangle = \int (\Delta\nu)^2 f(\nu)d\nu / \int f(\nu)d\nu$	
			Theory	Experiment
$0\gamma H_0(\perp)$	$\langle(\Delta H)^2\rangle_{av}/H_0^2$ ^{a, b, c}	Fig. 6	$0.64\langle(\Delta\nu)^2\rangle$ ^{f, g} $\sim\langle(\Delta\nu_0)^2\rangle$ ^b	0.7 to $1.5\langle(\Delta\nu_0)^2\rangle$
$0\gamma H_0(\parallel)$	$0.3\langle(\Delta H)^2\rangle_{av}/H_0^2$ ^a	Fig. 6	$\sim\frac{1}{2}\langle(\Delta\nu_0)^2\rangle$ ^{a, h}	Note h.
$\gamma H_0(\perp)$	$1 - (5/3)\langle(\Delta H)^2\rangle_{av}/H_0^2$ ^{d, e}	Reference line	$\langle(\Delta\nu_0)^2\rangle$ ⁱ	$(0.82 \pm 0.2)\langle(\Delta\nu_0)^2\rangle$
$\gamma H_0(\parallel)$	$\frac{2}{3}\langle(\Delta H)^2\rangle_{av}/H_0^2$ ^{a, d}	$(0.65 \pm 0.15)\langle(\Delta H)^2\rangle_{av}/H_0^2$	$0.77\langle(\Delta\nu_0)^2\rangle$ ^f	$(1.0 \pm 0.3)\langle(\Delta\nu_0)^2\rangle$
$2\gamma H_0(\perp)$	$\frac{2}{3}\langle(\Delta H)^2\rangle_{av}/H_0^2$ ^{b, d}	$(0.65 \pm 0.15)\langle(\Delta H)^2\rangle_{av}/H_0^2$	$1.13\langle(\Delta\nu_0)^2\rangle$ ^f	$(1.3 \pm 0.3)\langle(\Delta\nu_0)^2\rangle$
$2\gamma H_0(\parallel)$	$\frac{2}{3}\langle(\Delta H)^2\rangle_{av}/H_0^2$ ^{a, d}	$(0.70 \pm 0.15)\langle(\Delta H)^2\rangle_{av}/H_0^2$	$1.39\langle(\Delta\nu_0)^2\rangle$ ^f	$(1.5 \pm 0.3)\langle(\Delta\nu_0)^2\rangle$
Zero-field line	1	1.2 ± 0.25	$(10/3)\langle(\Delta\nu_0)^2\rangle$	$(10/3 \pm 0.5)\langle(\Delta\nu_0)^2\rangle$ ⁱ

^a A. Wright, Phys. Rev. **76**, 1826 (1949).
^b L. J. F. Broer, Physica **10**, 801 (1943).
^c $\langle(\Delta H)^2\rangle_{av} = \frac{2}{3}g^2\beta^2S(S+1)\sum_j r_{ij}^{-6}$.
^d L. Brown, IBM Research Laboratory, San Jose, California, Report (unpublished).
^e $\int f(\nu)d\nu$ is normalized to one for this line in the limit of large H_0 .
^f H. Cheng, Phys. Rev. **123**, 1359 (1961).
^g $\langle(\Delta\nu)^2\rangle = \frac{2}{3}g^4\beta^4k^{-2}S(S+1)\sum r_{ij}^{-6} = g^2\beta^2h^{-2}\langle(\Delta H)^2\rangle_{av}$.
^h This calculation by Wright was for spin $\frac{1}{2}$ and for only one crystalline orientation. Figure 6 indicates that if the lower frequency part of the line is excluded, the second moment is about the same as that of the $(0\gamma H_0 \perp)$ line.
ⁱ J. H. Van Vleck, Phys. Rev. **74**, 1168 (1948).
^j A. G. Anderson, Phys. Rev. **115**, 863 (1959).

it is held for a time, T_0 , short compared to T_1 . During the time T_0 , the sample which has been adiabatically cooled to a spin-system temperature, T_s , lower than the lattice temperature, T_L , is warmed by absorption of energy from the ac field. At the conclusion of the T_0 period, the spin system is adiabatically remagnetized to high field and a measurement of the spin system energy is made; this energy, $E_s(H_{0z})$, is directly proportional²¹ to the low-field spin system energy at the conclusion of the T_0 period and thus provides a measure of the absorption of energy which has occurred at low field. As Ramsey and Pound¹⁷ have pointed out, this method offers the sensitivity obtainable at high field and high frequency for analysis of phenomena taking place at low field and low frequency. The use of 270-cps modulation and lock-in techniques allows one to obtain sizable signal-to-noise ratios at 1 to 4.2°K (T_1 for²⁰ $\text{Li}^{7-} = 44$ sec at 1°K) at a resonance frequency of 1 Mc/sec. The dc field²⁰ is provided by a liquid-nitrogen-cooled air core solenoid driven by relays and having a transistor sweep supply. Samples were located in an rf head having three mutually perpendicular coils, the high-field receiver coil, the high-field transmitter (or low field \perp) coil, and the high-field modulation (or low field \parallel) coil.

Lithium dispersions, of $\geq 99.8\%$ purity, were obtained from the Lithium Corp. of America; copper samples of 99.999% purity were obtained from A. D. Mackay Co. and were powdered by filing; the Li-Mg alloys were obtained from W. D. Knight and prepared by dispersing in mineral oil. Particle sizes were in each case of the order of 10^{-3} in. in diameter.

Consider the experimental method; if it is assumed that $T_0 \ll T_1$, then the rate of energy change of the spin system at field H_0 upon application of field,

$H_{ac} \cos(2\pi\nu t)$, is given by

$$\frac{dE_s(H_0, t)}{dt} = A_0(\nu, H_0) \frac{H_{ac}^2}{T_s} = - \frac{A_0(\nu, H_0)}{E_0(H_0)} H_{ac}^2 E_s(H_0, t), \quad (6)$$

where $A_0(\nu, H_0)$ is the energy absorption per unit time per unit ac field at a spin system temperature of 1°K, and $E_0(H_0)$ is the energy of the spin system at 1°K; $E_s(H_0)$, of course, contains a factor T_s^{-1} . From (6) the change of E_s with time is exponential with a time constant

$$T_1' = |E_0(H_0)| / [A_0(\nu, H_0) H_{ac}^2].$$

Since $E_s(H_{0z})$ at H_{0z} (Fig. 1), is related to $E_s(H_0)$ by

$$\frac{E_s(H_{0z}, T_0)}{E_s(H_0, T_0)} = \{ [H_{0z}^2 + (5/3)\langle(\Delta H)^2\rangle] / [H_0^2 + (5/3)\langle(\Delta H)^2\rangle] \}^{\frac{1}{2}},$$

for a simple paramagnetic substance such as used here, the value of T_1' , and thus of $A_0(\nu, H_0) / |E_0(H_0)|$, may be readily measured by varying H_{ac}^2 and T_0 . Corrections for the case where T_1 is not large compared with T_0 are readily made.²¹ Now, $A(\nu, H_0)$ is given by the product of the distribution function $f(\nu)$, the energy per photon, the ac energy density, and the Boltzmann distribution of population by²

$$A(\nu, H_0) = \pi\chi''\nu H_{ac}^2 = (\pi^2/2kT_s)\nu^2 f(\nu) H_{ac}^2. \quad (7)$$

This has several experimental implications: First, if $f(\nu)$, for $H_0=0$, is a Gaussian, then the measured quantity is proportional to $\nu^2 \exp(\nu^2/2\nu_0^2)$, as was previously found, both theoretically and experimentally,⁸ to be the case for sodium. Figure 2 shows this ν^2 dependence for lithium at zero field and for frequencies small compared to ν_0 (~ 6 kc/sec) where $f(\nu)$ is expected⁸ to be constant. Second, the ν^2 factor in $A(\nu)$ tends to emphasize the wings of the absorption at $H_0=0$ to a larger extent than is the case at $H_0 \neq 0$, a

²¹ L. C. Hebel and C. P. Slichter, Phys. Rev. **113**, 1504 (1959).

TABLE II. Field dependence of A_0/E_0 at high field.

Line	$0\gamma H_0(\perp)$	$0\gamma H_0(\parallel)$	$\gamma H_0(\perp)$	$\gamma H_0(\parallel)$	$2\gamma H_0(\perp)$	$2\gamma H_0(\parallel)$
$[A_0(H_0)/E_0(H_0)]_{\max}$ field dependence	$\propto 1/H_0^4$	$\propto 1/H_0^6$	constant	$\propto 1/H_0^2$	$\propto 1/H_0^2$	$\propto 1/H_0^2$

fact that has implications for the observation of quadrupole broadening of zero-field spectra. Third, since $[f(\nu)]_{\max}$ for the $0\gamma H_0$ line (assuming constant linewidth) varies as H_0^{-2} for the perpendicular case and as H_0^{-4} for the parallel case, and since $E_0(H_0)$ varies as $\chi_0 H_0^2$, the experimentally observed quantity $(A_0/E_0)_{\max}$ varies as either H_0^{-4} or H_0^{-6} in the high-field limit. Similar considerations hold for other lines, again assuming that the lines are of fixed width.⁹ The $\gamma H_0(\perp)$ line, the Larmor line, is the only line which has $(A_0/E_0)_{\max}$ independent of field in the high-field limit; this happens because $[f(\nu)]_{\max}$ is independent of field for this line and the ν^2 factor in A_0 cancels out the H_0^{+2} dependence in E_0 . The field dependences of A_0/E_0 for the maxima of the various lines are listed in Table II; the work of Cheng,⁹ Wright,⁵ and Van Vleck¹⁰ has established the invariance of linewidth with change in field H_0 , for H_0^2 large compared with $\langle \Delta H^2 \rangle$. This table indicates the difficulty which one would have in experimentally following the $0\gamma H_0$ lines out to large values of H_0 ; one is, in fact, limited in the values of H_{ac} which can be applied, since at $H_{ac}^2 \sim \langle \Delta H^2 \rangle$ one would expect departures from applicability of the present theory. Finally, (6) and (7) indicate a linear dependence of A/E on H_{ac}^2 which should hold as long

as the spin system attains equilibrium in times short compared with T_0 . Figure 3, in which T_1' is plotted against H_{ac}^{-2} , shows a typical case of this H_{ac}^2 dependence. Although the dependence of the absorption upon both ν^2 (Fig. 2) and H_{ac}^2 (Fig. 3) has been observed in spin-spin relaxation in electron paramagnetic systems for some time,² the data in the nuclear magnetic case are included here to illustrate the experimental method and to demonstrate its applicability to this problem.

So far, both theory and experimental method have assumed equilibrium within the spin system at a spin temperature T_s . In situations where either power is being supplied to the system or $H_0^2 \gg \langle \Delta H^2 \rangle$, it is not too surprising that observable departures from equilibrium occur. A departure from H_{ac}^2 dependence of the absorption was found repeatedly in the Larmor line, $\gamma H_0(\perp)$, at fields above about 12 gauss for lithium, with T_0 's of the order of seconds. This type of effect, not present at the lower fields, is believed to be similar to the effects considered by Redfield²² at considerably higher fields, where, for $H_{ac} > (\gamma^2 T_1 T_2)^{1/2}$, nonsaturation of the dispersion occurs. A second effect observed in the $0\gamma H_0(\parallel)$ line is an additional absorption at low frequency as a result of nonequilibrium between Zeeman and spin-spin energies. These frequencies are typically of the order of hundreds of cycles per second at a 10-gauss field.

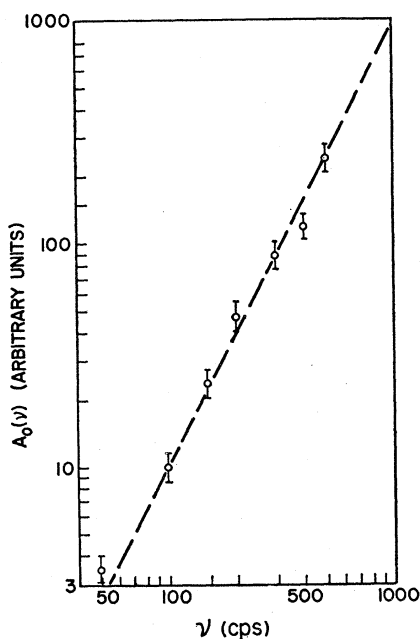


FIG. 2. Spin absorption frequency dependence of the zero-field line in lithium. The energy absorbed per unit time, $A(\nu)$, is expected to be proportional to ν^2 at the low-frequency end of the spectrum. The dashed line indicates the ν^2 dependence; the experimental points fall quite well along this line.

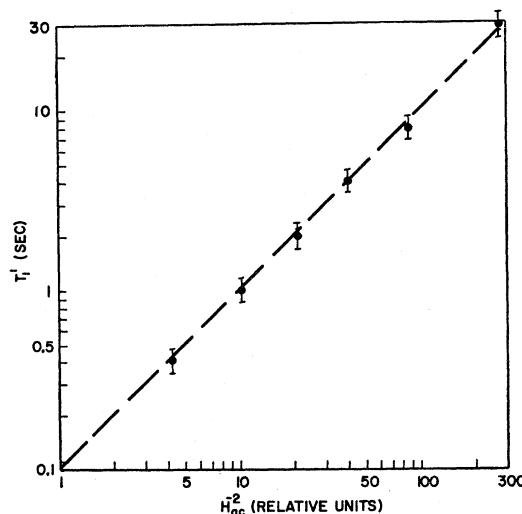


FIG. 3. Dependence of T_1' , the relaxation time with ac field applied [Eq. (6)], upon the ac magnetic field amplitude. This shows the linear dependence of T_1' upon H_{ac}^{-2} for the zero-field line. (The units of H_{ac}^{-2} are chosen to give $T_1' = 0.1$ sec at $H_{ac}^{-2} = 1.0 \text{ Li}^2$ at 8 kc/sec).

²² A. G. Redfield, Phys. Rev. **98**, 1787 (1955).

IV. EXPERIMENTAL RESULTS AND DISCUSSION

A. The Larmor Line, $\gamma H_0(\perp)$

The experimental quantity $(A_0/E_0)_{\max}$ is independent of field over the range of 7 to 12 gauss for Li^7 , in agreement with Table II, within an accuracy of $\pm 10\%$.

As a check on the method, the second moment of the Larmor line was measured for Li^7 (Table I). To make this measurement, $f(\nu) = A(\nu)\nu^{-2}$ must first be determined and then the second moment of this line found. Accuracy of this second moment measurements is about $\pm 20\%$ here, and the result in this case is in reasonable agreement with the theory.

At dc fields above 12 gauss it is observed that nonlinear power dependences of the absorption occur at H_{ac} fields which are small compared with ΔH . The effect is particularly marked near the center of the absorption line. Redfield²² has shown that for high enough H_0 fields (and large enough H_{ac}) the magnetization "locks in" along the direction of the effective field, in the frame rotating at angular frequency $2\pi\nu$. In this case, absorption of energy ceases to be proportional to H_{ac}^2 . This is what is believed to be happening here at dc fields above 12 gauss. At lower fields, the nonsecular terms neglected by Redfield apparently provide strong enough coupling between spin-spin and Zeeman energies that such effects are negligible. This assumption is not unreasonable, since the nonsecular terms neglected by Redfield include those which provide exchange of spin-spin and Zeeman energies, a process which has a relaxation time¹² of order $T_2' = T_2 \exp\{H_0^2/2(\delta H)^2\}$, where $(\delta H)^2$ is of the order of the second moment, $\langle(\Delta H)^2\rangle$; for lithium T_2' will be of the order of seconds at $H_0 \approx 10$ to 20 gauss.

These considerations indicated that it should be possible to perform adiabatic fast passage down to rather low fields and that in the low-field limit, when T_2' becomes small, the fast passage technique could be expected to fail. An experimental check²³ of this showed that adiabatic fast passage worked well down to dc fields of about 12 gauss for Li^7 , below which it was possible to observe only saturation in a 50-msec pass through the line.

The integrated intensity of the Larmor line is the standard by which the other lines of Table I were measured, so its relative intensity is listed simply as 1.0.

B. Second Harmonic Line in Perpendicular Field, $2\gamma H_0(\perp)$

This line arises from the H_5 and H_6 contributions to the Hamiltonian (1) and in particular from the fact that $\sum I_{+i}I_{zj}$, together with the applied ac field, makes possible double spin flips giving absorption at $2\gamma H_0$. Figure 4 shows spectra obtained for lithium at fields of about 10 gauss. The second harmonic line is

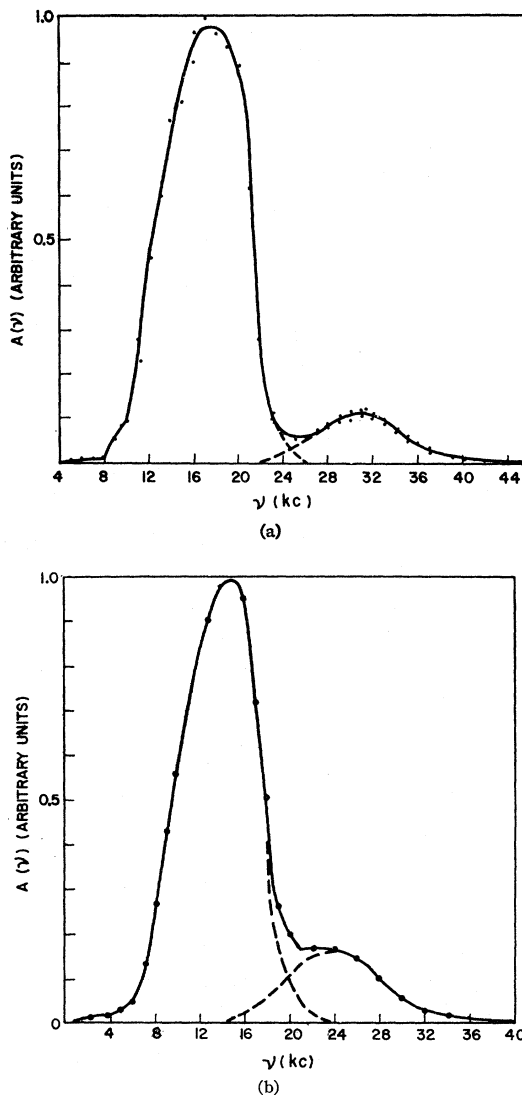


FIG. 4. Spectra of Li^7 for the perpendicular-field case. In (a) the field is 10 gauss, while in (b) the field is 8 gauss.

considerably smaller than the Larmor line, but is fairly well resolved. Analysis of these data gives the $2\gamma H_0(\perp)$ result in Table I. The ratio of its amplitude to that of the Larmor line and the field dependence of the line are in good agreement with theory. Nonlinear power effects were not observed here. The second moment of this line about its center has limitations on its accuracy arising from the necessity to eliminate contributions to the wings from the Larmor line on the low-frequency side and from the $3\gamma H_0(\perp)$ line on the high-frequency side. The separation is done with the assumption of Gaussian tails for amplitudes of less than two-tenths of the peak line amplitude. Within these limitations, however, the agreement with Cheng's work is reasonable, giving a slightly greater width for this line than for the Larmor line itself.

²³ A. G. Anderson (to be published).

C. The First and Second Harmonic Lines in Parallel Field, $\gamma H_0(\parallel)$, $2\gamma H_0(\parallel)$

The $\gamma H_0(\parallel)$ line arises from the H_5 and H_6 terms in the Hamiltonian in conjunction with an ac field along the z axis of (1), while the $2\gamma H_0(\parallel)$ line arises from the ac and the H_3 and H_4 terms. Both lines are proportional in amplitude to H_0^{-2} . Figure 5 shows some of the parallel-field spectra for lithium with a plot of $f(\nu)$ and $A(\nu)$ vs frequency for fixed field. In the $A(\nu)$ curves the $2\gamma H_0(\parallel)$ line is considerably larger, as it should be, since for fixed field the $\int f(\nu)d\nu$ (Table I) is the same for both and $A \propto \nu^2 f(\nu)$, which would indicate a relative ratio of total absorption of 4×1 , about as observed. In the $f(\nu)$ data the spectrum is broken down into its contributions from $0\gamma H_0(\parallel)$, $\gamma H_0(\parallel)$, and $2\gamma H_0(\parallel)$ lines by assuming that the $2\gamma H_0(\parallel)$ and $\gamma H_0(\parallel)$ lines are symmetrical with Gaussian tails.

These lines suffer from the same errors with respect to measurement of second moment as was the case in the $2\gamma H_0(\perp)$ line. The $2\gamma H_0(\parallel)$ line could be and was resolved somewhat better by working at higher field; unfortunately, the experimental arrangement was such that at higher fields contributions to the $\gamma H_0(\parallel)$ line from the $\gamma H_0(\perp)$ line were difficult to minimize. The field dependence, total intensity, and second moment of both lines is in good agreement with theory within these experimental limitations. Relative values of ac fields in perpendicular- and parallel-field cases were obtained by comparison of absorption at zero field.

It is of interest to note that the relative amplitudes of $A(\nu)$ for the γH_0 and the $2\gamma H_0$ lines in Fig. 5 are interchanged, and the $2\gamma H_0$ line appears half as wide if one plots a fixed frequency-variable field absorption spectrum, as is the experimental arrangement for the work at 9 kMc/sec of Kutuzov and Kurushin.⁶

D. Zero Frequency Lines, $0\gamma H_0(\perp)$, $0\gamma H_0(\parallel)$

Theory⁹ shows from (1) that the $0\gamma H_0(\perp)$ line arises from the terms H_5 and H_6 and the x -axis ac field and has a field dependence proportional to H_0^{-2} . There are no terms in (1), in first-order perturbation, which give a line for $0\gamma H_0(\parallel)$, while in the next order of perturbation such terms arise from combinations of H_3 , H_4 , and the ac field or H_5 , H_6 , and the ac field; a line is obtained which is proportional to H_0^{-4} . The ratio, δ , of $[0\gamma H_0(\parallel)]/[0\gamma H_0(\perp)]$, assuming comparable line-width and shape, as the calculations of Wright⁵ indicate, should thus be proportional to H_0^{-2} at high field. At zero field this ratio is clearly equal to one, while at low field, where $H_0^2 \ll (10/3)\langle \Delta H^2 \rangle$, δ should be only slightly field dependent. These requirements are satisfied by the choice of a function $A^2(A^2 + H_0^2)^{-1}$ for δ , where one expects that a reasonable value of A^2 should be one of the order of $(10/3)\langle \Delta H^2 \rangle$. Figure 6 shows the experimental data for δ in Li^7 , together with a comparison for $A^2 = (10/3)\langle \Delta H^2 \rangle$. Actually, the exact value of A^2 is not too meaningful without more detailed calculations

for the $0\gamma H_0(\parallel)$ line. The high-field behavior of δ demonstrates, however, the expected H_0^{-2} variation for frequencies greater than 500 cps or so. The H_0^{-2} and

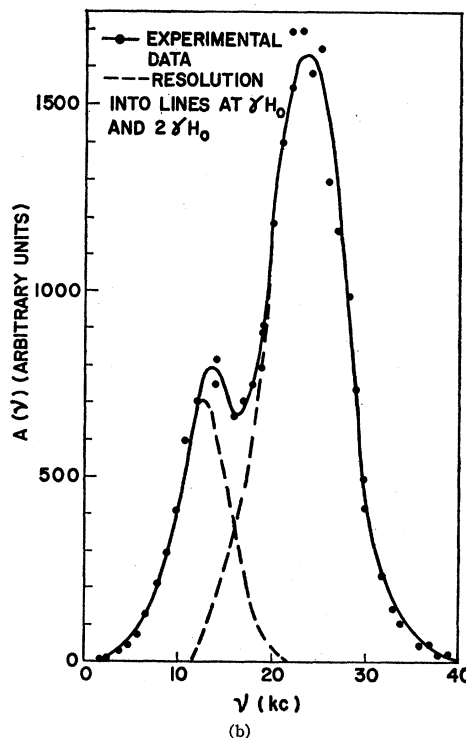
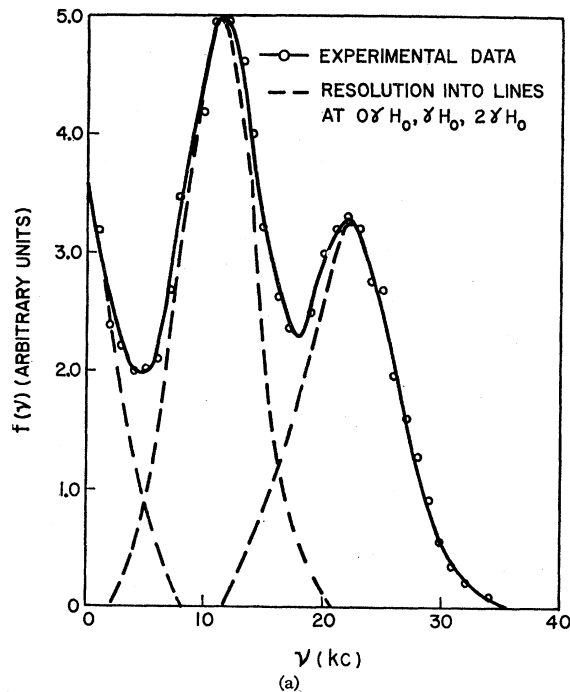


Fig. 5. Spectra for Li^7 in the parallel-field case at 7 gauss. In (a) the spectrum of $f(\nu)$ is shown, while in (b) the spectrum of $A(\nu)$ is shown. The relative values of $\int f(\nu)d\nu$ in (a) for $\gamma H_0(\parallel)$ and $2\gamma H_0(\parallel)$ is 1 to 1, while in (b) the relative values of $\int A(\nu)d\nu$ are 1 to 4.

TABLE III. Zero-field spectra in Li-Mg alloys.

Sample ^a	$\langle(\Delta\nu)^2\rangle$ Total (kc/sec) ²	$\langle(\Delta\nu)^2\rangle_{dd}$ (kc/sec) ²	$\langle(\Delta\nu)^2\rangle_Q$ (kc/sec) ²
Li ⁷	38	38	...
Li-Mg (96.15% Li)	45	38	7
Li-Mg (80.9% Li)	64	36	28
Li-Mg (55.6% Li)	79	32	47

^a Percentages given for Li are by weight.

H_0^{-4} dependences of $\int f(\nu)d\nu$ were also checked by direct measurements on each line.

Figure 7 shows experimental data for the $0\gamma H_0(\parallel)$ and $0\gamma H_0(\perp)$ lines, $f(\nu)$, at a field of about 7 gauss. The rise in both lines at 6 kc/sec indicates the onset of absorption due to the Larmor line, a contribution which leads to the relatively large uncertainty in the second moment measured.

A striking feature of the parallel-field data is the enhanced absorption at low frequencies. This low-frequency peaking develops continuously with field, starting from zero field where it is not observed and becoming noticeable for dc fields above 5 gauss or so, after which it assumes the character shown in Fig. 7. The theory of absorption in this case has been treated in detail by Caspers and others. An additional low-frequency absorption occurs when the time for equilibrium within the spin system, T_2' , becomes long. In this case the susceptibility no longer follows the applied ac field, and a "relaxation" absorption occurs at frequencies of the order of $(T_2')^{-1}$. The time for equilibrium within the spin system¹² is given by a function of order $T_2' = T_2 \exp(C^2 H_0^2)$, where C^2 is of the order of $[(10/3)\langle(\Delta H)^2\rangle]^{-1}$ and T_2 is the conventional zero-field spin-spin relaxation time. If one assumes a Lorentzian distribution function for the enhanced absorption, then the absorption $\chi'' \approx \nu f(\nu)$ peaks at a frequency of $\omega = (T_2')^{-1}$. For Li⁷ and a C^2 of $[(10/3)\langle(\Delta H)^2\rangle]^{-1}$, $H_0 \approx 10$ gauss, the frequencies involved are of the order of 100 cps, in reasonable agreement with Fig. 7. Further details of this enhanced absorption are being studied and will be reported separately.²³

E. Absorption Spectra of Li-Mg Alloys

The zero field spectra for Li-Mg alloys are compared in Fig. 8. Table III summarizes the second-moment values obtained and the quadrupole contributions to these second moments obtained from a separation given by (5). The magnitude of these quadrupole interactions is in good agreement with the data of Sukenik,¹⁶ but in substantial disagreement with the data of Weinberg.²⁴ Both of these authors took their data at high field and relatively higher temperatures. Since lithium has a small antishielding factor, γ_∞ , it does not appear likely that the quadrupole interactions are large, as Wein-

²⁴ D. L. Weinberg (to be published).

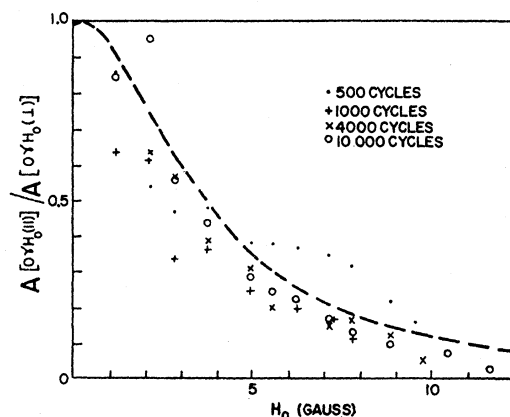


FIG. 6. The quantity $A[0\gamma H_0(\parallel)]/A[0\gamma H_0(\perp)]$ plotted as a function of field. Since the theoretical absorption for the parallel-field case decreases as H_0^{-4} and the absorption for the perpendicular case decreases as H_0^{-2} , the theoretical dependence for this ratio, in the limit of high field, is proportional to H_0^{-2} . The dashed curve is a plot of $14(H_0^2 + 14)^{-1}$.

berg's data would indicate, nor does it appear likely that precipitation occurs at these relatively low concentrations of Mg. Knight²⁵ has considered theoretically the magnitude of the quadrupole interactions and has found reasonable agreement between the magnitude of quadrupole interactions due to both charge and lattice distortion and the magnitudes reported here.

Figure 9 compares the $A(\nu)$ of Li⁷ and Li⁷-Mg for the $\gamma H_0(\perp)$ and $2\gamma H_0(\perp)$ lines at a field of about 10 gauss. The theory shows, from (5), that the $\gamma H_0(\perp)$ line

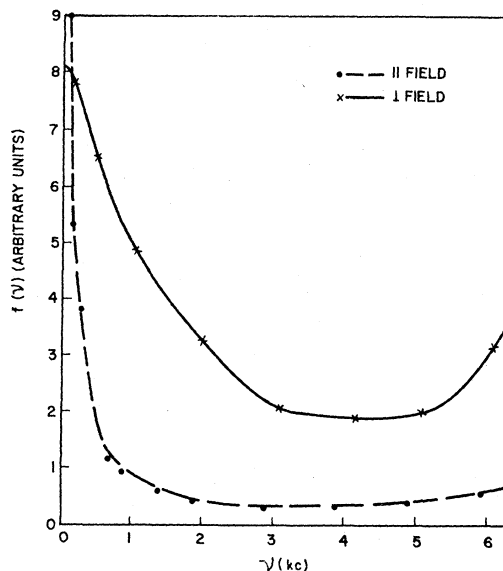


FIG. 7. The distribution function $f(\nu)$ at $H_0 = 7$ gauss for $0\gamma H_0(\parallel)$ and $0\gamma H_0(\perp)$. The shape of the $0\gamma H_0(\perp)$ line is relatively insensitive to dc field. Note, however, the sharp peak in the parallel-field case which is produced by the internal time constant for exchange of Zeeman and dipole-dipole energy; the shape of this line varies rapidly with variation of the dc field.

²⁵ W. D. Knight (private communication).

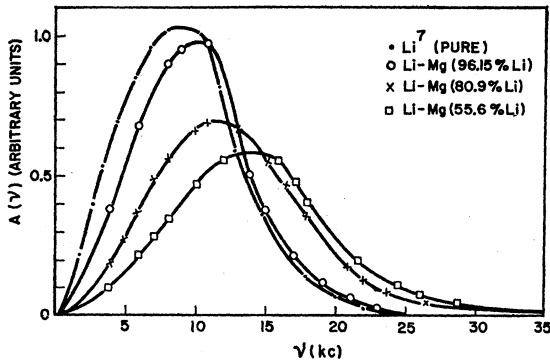


FIG. 8. The zero-field absorption spectrum, $A(\nu)$, for lithium-magnesium alloys. The percentages given for lithium are by weight. The spectrum is obtained by observation of the Li^7 absorption at high field (Fig. 1).

should be broader and the $2\gamma H_0(\perp)$ line larger in amplitude for the alloy, in agreement with Fig. 9. These spectra can also be used to obtain the quadrupole interaction, but the zero-field spectra are somewhat simpler to analyze.

Experimental results also show that the $0\gamma H_0(\perp)$ line falls off more slowly with H_0 in the alloys than in the pure metal. This is also expected, and was predicted long ago⁴; it occurs because of the increased "effective second moment" of the line.

A check of the T_1 for the 18 at. % Mg alloy gave a T_1 (Li^7 in Li-Mg) = $1.15 \pm 0.05 T_1$ (Li^7), in reasonable agreement with a linear extrapolation of Knight shift data.²⁶

Lithium-magnesium alloys represent an ideal case for

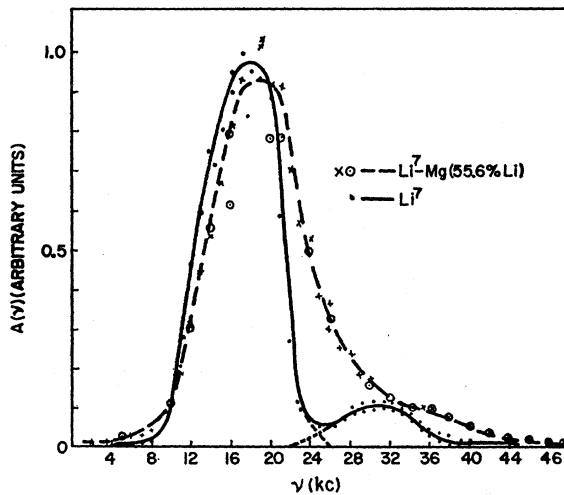


FIG. 9. Comparison of the perpendicular-field absorption spectrum (at 10 gauss) for pure lithium metal and for a lithium-magnesium alloy of 55.6% (by weight) lithium.

²⁶ D. G. Hughes, *Phil. Mag.* 5, 467 (1960).

observation of the mixed quadrupole and magnetic dipole interactions because these interactions are of roughly the same magnitude. Consequently, the whole spin system is tightly coupled at low field, a fact that is verified by the linear power dependence of the observed absorption. Unfortunately, extensions of the same technique to other cases, such as Al-Mg, have indicated that, in situations where the quadrupole interaction is large compared with the dipole-dipole interaction, the spin temperature approximation breaks down. In this case, it was found that the entire zero-field spectrum could not be saturated by application of power to a part of the spectrum, as is the case in a tightly coupled system with a unique T_s . It may be possible to minimize difficulties by working in a temperature region (long T_1) where the time spent at zero field is long enough for equilibrium to occur; the latter time can be very long indeed for large quadrupole interactions.

F. Zero-Field Line of Copper

The zero-field spectrum for copper, shown in Fig. 10, was obtained by observing Cu^{63} at high field. The

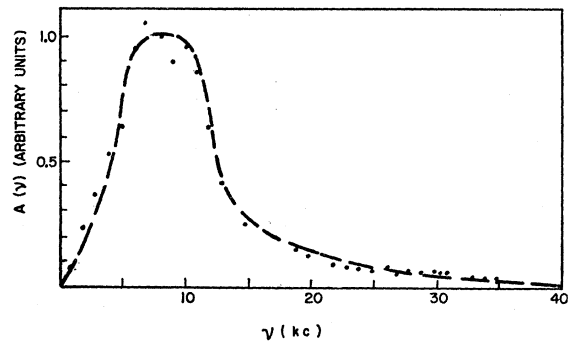


FIG. 10. Zero-field spectrum, $A(\nu)$, of copper. The experimental second moment is higher, by a factor of 1.6, than the theoretical value, most probably due to residual quadrupole interactions.

particular spectrum shown was for 99.999% pure copper, which had been filed and annealed in vacuum. Interestingly enough, it was found that the same spectrum was also obtained for samples which had not been annealed after filing, although considerable zero-field broadening might have been expected in this case.¹⁶ Measurements at room temperature (and at 77°K) and high field showed little difference between the line shapes and amplitudes of the two samples, although an alloy of $\frac{1}{8}$ at. % silver-copper showed the expected reduction in line amplitude. Apparently the quadrupole interactions reported by Bloembergen and Rowland¹⁶ are not particularly important in "as filed" specimens of this high purity. The zero-field linewidth observed

is about 36 (kc/sec)^2 , about 1.6 times as large as the theoretical value for dipole-dipole interaction alone.

V. CONCLUSIONS

The work reported here indicates agreement between theory and experiment for a number of the satellite lines in lithium metal. The method appears to be applicable to a number of problems, including some of those involving quadrupole interactions in alloys.

ACKNOWLEDGMENTS

The author would like to thank E. Benton for some of the high-field work on copper reported here, and to acknowledge his assistance and that of H. Lee in the performance of the experimental work. Conversations with A. G. Redfield and Professor W. Knight, Professor A. Portis, and Professor E. Hahn were both stimulating and helpful.

Far-Infrared Ferroelectric Vibration Mode in SrTiO_3 †

A. S. BARKER, JR., AND M. TINKHAM

Department of Physics, University of California, Berkeley, California

(Received October 30, 1961)

The real and imaginary parts of the dielectric constant of SrTiO_3 have been obtained for the region 2.5 to 3000 cm^{-1} from an analysis of the reflectivity. The imaginary part exhibits a very strong peak at 100 cm^{-1} at room temperature which shifts to 40 cm^{-1} at 93°K . This mode is of sufficient strength to account for more than 90% of the low-frequency dielectric constant. The accompanying dispersion of the real part of the dielectric constant is of resonant form. The connection of this mode with Cochran's theory of ferroelectricity is discussed.

I. INTRODUCTION

THE low-frequency dielectric constant of ferroelectric crystals is well known to obey a Curie law $\epsilon' = C/(T - T_c)$ for temperatures above a certain critical temperature which is usually very close to T_c . Values of ϵ' can be as large as 10^6 . One of the Kramers-Kronig relations provides a connection between the behavior of the imaginary part of the dielectric constant and the low-frequency real part:

$$\epsilon'(0, T) - \epsilon_\infty = \frac{2}{\pi} \int_0^\infty \frac{\epsilon''(\omega', T) d\omega'}{\omega'} \quad (1)$$

Here $\epsilon'(\omega, T)$ and $\epsilon''(\omega, T)$ are the real and imaginary parts of the dielectric constant and ϵ_∞ is the limiting dielectric constant for frequencies well above those where ferroelectric effects cease to be important. The value of ϵ'' in the integral is understood to include only contributions from modes in the frequency region of interest. For SrTiO_3 at room temperature the left side of (1) is about 300 and follows a Curie law behavior [ϵ_∞ can be neglected compared with $\epsilon'(0, T)$]. For the alkali halides or quartz the value of $\epsilon'(0, T) - \epsilon_\infty$ is 3 or 4 and is temperature insensitive. The point of interest is that previous spectroscopy of SrTiO_3 and related ferroelectrics has yielded an ϵ'' very little different from that of the alkali halides or quartz in terms of its contribution to $\epsilon'(0, T)$ via (1). Recently

Cochran¹ has proposed a theory of ferroelectricity which associates the ferroelectric transition in certain crystals with one of the optic modes of the lattice lowering its frequency and becoming unstable as the temperature is lowered toward T_c . Others, particularly P. W. Anderson, had discussed similar ideas previously in unpublished work. This paper reports a Cochran-type mode in SrTiO_3 whose contribution to ϵ'' satisfies (1) and which provides a resonant dispersion of ϵ' .

II. EXPERIMENTAL WORK

The reflectivity of strontium titanate has been measured over the range 2.5 to 250 cm^{-1} at 93°K and from 2.5 to 3000 cm^{-1} at 300°K . Figure 1 shows the

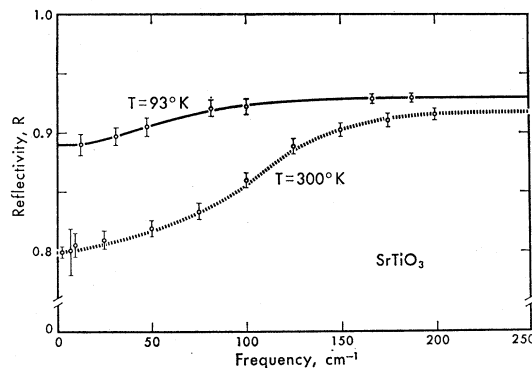


FIG. 1. Reflectivity of SrTiO_3 in the far infrared. The smooth curves are used in the dispersion analysis.

† Supported in part by the Office of Naval Research, the National Science Foundation, and the Alfred P. Sloan Foundation.

¹ W. Cochran, *Advances in Physics*, edited by N. F. Mott (Taylor and Francis, Ltd., London, 1960), Vol. 9, p. 387.